Available online at www.sciencedirect.com
ScienceDirect
Acta Biomaterialia 4 (2008) 1038–1045
Acta BIOMATERIALIA
www.elsevier.com/locate/actabiomat

Drug release behavior of chitosan–montmorillonite nanocomposite hydrogels following electrostimulation

Kun-Ho Liu, Ting-Yu Liu, San-Yuan Chen *, Dean-Mo Liu *

Department of Materials Science and Engineering, National Chiao-Tung University, 1001 Ta-hsueh Road, Hsinchu, Taiwan

Received 16 September 2007; received in revised form 11 December 2007; accepted 23 January 2008
Available online 8 February 2008

Abstract

Nanocomposites hydrogel (nanohydrogel) composed of chitosan (CS) and montmorillonite (MMT) were prepared and systematically studied for drug release behavior following electrostimulation. The deterioration of the responsiveness and reversibility of CS upon repeated on–off electrostimulation switching operations are major limitations for clinical applications, as it suffers from too much structural instability for the precise control of the release of drug upon cyclic electrostimulation. To overcome these limitations, an inorganic phase, MMT, was incorporated in the CS matrix to enhance the anti-fatigue property and corresponding long-term stable release kinetics. X-ray diffraction analysis and time-dependent optical absorbance showed that the MMT incorporated into the nanohydrogel exhibited an exfoliated nanostructure. The exfoliated silica nanosheets are able to act as cross-linkers to form a network structure between the CS and MMT, and this difference in the cross-linking density strongly affects the release of vitamin B_{12} under electrostimulation. With a lower MMT concentration (1 wt.%), the release kinetics of vitamin B_{12} from the nanohydrogel shows a pseudo-zero-order release, and the release mechanism was changed from a diffusion-controlled mode to a swelling-controlled mode under electrostimulation. Further increasing the MMT content reduced both the diffusion exponent n and the responsiveness of the nanohydrogel to electrostimulation. In addition, a consecutively repeated "on" and "off" operation shows that the electroresponsiveness of the nanohydrogel with higher MMT concentrations was reduced, but its anti-fatigue behavior was considerably improved. In this work, the nanohydrogel with 2 wt.% MMT achieved a mechanically reliable and practically desirable pulsatile release profile and excellent anti-fatigue behavior, compared with that of the pure CS.

Keywords: Chitosan; Montmorillonite; Nanocomposite hydogel; Electrostimulation controlled release; Anti-fatigue

1. Introduction

Smart polymer hydrogels have been studied with particular emphasis on their reversible volume changes in response to external stimuli, such as pH, solvent composition, temperature, ionic concentration and electric field [1–3]. These hydrogels have been developed and studied with regard to their application in several biomedical fields, e.g. separation techniques, soft-actuators and controlled drug delivery systems [4,5]. Of these, their use in electrically controlled drug delivery may offer unique advantages for providing on-demand release of drug molecules from implantable reservoirs. In addition, electrical control is advantageous for coupling to sensors and microelectronics in feedback controlled systems [6].

For electrosensitive hydrogels used as controlled drug delivery systems, the drug release rate can be easily controlled simply by modulating the electric field. Generally, the extent of drug release increases with the magnitude of electric field and time, but is not linearly proportional to them [7]. Hence, it becomes more difficult to precisely control the release of drug by electrostimulation. In particular, an important goal of drug delivery is to obtain a constant release rate for a prolonged time. However, one problem

* Corresponding authors. Tel.: +886 3 5731818; fax: +886 3 5725490.
E-mail addresses: sanyuanchen@mail.nctu.edu.tw (S.-Y. Chen), deanmo_liu@yahoo.ca (D.-M. Liu).

1742-7061/$ - see front matter © 2008 Acta Materialia Inc. Published by Elsevier Ltd. All rights reserved.
doi:10.1016/j.actbio.2008.01.012

common to all hydrogels is that the responsiveness and reversibility will decrease after several on–off switching operations. For commercial applications, this fatigue property must be improved to achieve a stable pulsatile release under repeatedly operations. Unfortunately, few studies have addressed this important issue, so this is one of the research objectives of this investigation. In order to overcome the fatigue problem of conventional hydrogels to some extent, the incorporation of an inorganic nanophase is an attractive alternative, i.e. production of an inorganic–organic nanocomposite hydrogel (nanohydrogel), where the properties of polymer matrix could be improved and have a significant effect on the electrical deformation and relaxation behaviors [8]. For example, Gong et al. [9] reported that organically modified clay can enhance the temperature response of clay–poly(*N*-isopropylacrylamide) (PNIPAAm) nanocomposites. Based on hydration theory, the organically modified clay introduces a hydrophobic environment at the interface that can enhance the efficiency of the thermal transition, narrow the transition range and increase the transition rate. However, to the best of our knowledge, little research work had been reported on the drug release behavior of polymer–(nano)clay nanohydrogel following electrostimulation.

Polymer–clay nanohydrogels are expected to have novel properties because of the nanometric scale on which the nanoclay particles, with their plate-like shape, would alter the physical and chemical properties of the polymeric materials and improve their mechanical properties and thermal stability [10]. Chitosan (CS), which is used as polymeric matrix in this study, is a cationic biopolymer and has been proposed for electrically modulated drug delivery [11]. In our previous study [12], we demonstrated that the addition of clay to the CS matrix could strongly affect the cross-linking density as well as the mechanical property, swelling–deswelling behavior and fatigue property of the nanohybrids. Hence, the incorporation of negatively charged delaminated (exfoliated) montmorillonite (MMT) is expected to electrostatically interact with the positively charged $-NH^{3+}$ group of CS, to generate a strong cross-linking structure in the nanohydrogel [13] and, thus, strongly affect the macroscopic property of the nanohydrogel and the drug diffusion through the bulk entity. In present work, variations in the release kinetics and the mechanism of vitamin B_{12} action with respect to MMT content were investigated under a given electric-field stimulus. Furthermore, the anti-fatigue behavior with respect to the repeated field stimuli of the resulting nanohydrogel in terms of the MMT addition was also elucidated.

2. Materials and methods

2.1. Materials

The chitosan used in this study to prepare the CS–MMT nanohydrogels was supplied by Aldrich–Sigma and used without purification. The same type of chitosan was used by Darder et al., who reported that it has an average molecular weight of 342,500 g mol^{-1} and a deacetylation degree (DD) of ca. 75% [14]. Acetic acid and sodium phosphate for the preparation of buffers were purchased from Aldrich Chemicals. Vitamin B_{12} (Sigma–Aldrich Co.) was chosen as a model molecule to characterize the release behavior from the nanohydrogel. Na^+-montmorillonite, supplied by Nanocor Co., is an Na^+ form of layered smectite clay with a cationic exchange capacity (CEC) of 120 meq. $(100\ g)^{-1}$. The MMT platelet shows a surface dimension of about 200–500 nm in length and several tens of nanometers in width.

2.2. Preparation of CS–MMT nanohydrogels

To prepare the CS–MMT nanohydrogels, the preparation procedure is separated into two stages. The first stage is to prepare a suspension containing MMT and CS with a weight ratio of 1:2 (where the CS solution was prepared by dissolving predetermined amounts of CS in 1 wt.% acetic acid solution and stirring for about 4 h until the CS was completely dissolved). The CS–MMT suspensions were obtained by adding CS to an aqueous solution containing 2 wt.% MMT (i.e. 0.5 g of Na^+-MMT dispersed in 25 ml of double-distilled water), followed by stirring at 50 °C for 24 h. To enhance the formation of exfoliation of the MMT in the final nanohydrogel, the suspension with a CS to MMT ratio of 2:1 was then subjected to ball-milling for 24 h, after which the as-prepared final CS–MMT suspension was used to form nanohydrogel.

In the second stage of the CS–MMT nanohydrogel preparation, 2 wt.% CS solution was obtained by dissolving CS in 1 wt.% acetic acid solution. A small amount of the ball-milled CS–MMT suspension was then added to the prepared CS solution to form a CS-rich suspension, with the MMT content controlled in the range of 1, 2, 3 and 4 wt.%, relative to the total weight of CS in the suspensions, under continuous stirring at 60 °C for 1 h. This final suspension was then cast onto Petri dishes and dried at 30 °C for 24 h, to form final dried nanohydrogels. The dried nanohydrogels were then rinsed with an aqueous solution of 1 M NaOH to remove any residual acetic acid, followed by washing with distilled water and drying for 1 week at 40 °C in vacuum until use. The compositions of the nanohydrogels are expressed using the value of n to define the content of MMT in CS–MMTn, where $n = C_{MMT}$, the content of the MMT incorporated in the nanohydrogels, which ranged from 1% to 4%.

2.3. Characterization

The crystallographical structures of CS–MMT nanohydrogels were determined using an X-ray diffractometer (XRD; M18XHF, Mac Science, Tokyo, Japan). The diffraction data were collected from $2\theta = 1$–$30°$ at a scanning rate of $2°\ min^{-1}$. The nanohydrogel was a circular plate with a radius of about 1.5 cm. The average thickness and

weight of the nanohydrogel were measured to be 0.20 mm and 0.15 g, respectively. The stability of the CS–MMT suspensions was characterized using the optical absorbance of an ultraviolet–visible (UV–Vis) spectrometer (SP-8001, Metertech Inc.), at a wavelength of 550 nm. Square glass cuvettes with a path length of 1 cm were used as sample holders. All the data shown in the work are average values of three measurements and the measurement error is well below 5%.

2.4. Swelling under an applied voltage

The dry nanohydrogel, pre-equilibrated and swollen in 20 ml phosphate-buffered solution (PBS, pH 7.4) for equilibrium, was cut into circular plates (1 cm radius) and weighed. Two ring-shaped platinum electrodes (outer radius 1.5 cm and inner radius 0.5 cm) were kept in contact with the opposite surface of the swollen nanohydrogel in the PBS. An electric voltage of 5 V was applied from a DC power source for 1 h. After the excessive surface water had been removed with filter paper, the weight of the swollen samples was measured. The procedure was repeated three times, until no further weight gain could be detected. All the data shown are averages of three measurements, where the measurement error is well below 5%.

2.5. Drug release under an applied voltage

Prior to drying, 2% vitamin B_{12} (relative to the total weight of the final suspensions) was added to the final suspensions (prepared for forming nanohydrogel in the second stage). The drug-loading nanohydrogel, pre-equilibrated and swollen in 20 ml PBS for 5 min, was cut into a circular plate (radius of 1 cm) and weighed. Two ring-shaped platinum electrodes (outer radius 1.5 cm and inner radius 0.5 cm) were kept in contact with the opposite surface of the swollen nanohydrogel in the PBS, and an electric voltage of 5 V was applied as before [15]. At appropriate time intervals, 3 ml of solution was extracted from the container and analyzed using a UV spectrophotometer (Agilent 8453) at a specific wavelength of $\lambda = 361$ nm.

For on–off switching operation, the drug-loading nanohydrogel swollen in 20 ml PBS was kept in contact with two platinum electrodes for electrostimulation. A cyclic on–off switching operation was carried out for 10 cycles, with the time durations of the switching between "on" and "off" both being 5 min. The amount of drug release was measured spectroscopically at various time intervals. Since there is a risk of error in measuring the drug release rate between the different batches of drug loads in the nanohydrogels during the on–off operation, with the difference in drug concentration between each operation for different samples causing a variation (mostly a reduction) in the release rate in the later stages, we defined a standard release rate (R_{sd}) by normalization of the release rate upon each cycle of test:

$$R_{sd} = [(M_{i-1} - M_i)/M_{i-1}]/t, \quad i \geqq 1$$

Here, M_i is the residual drug amount in the nanohydrogel for the ith electrostimulation and t is the time of the applied voltage of 5 V (5 min). The obtained values are an average of three measurements and the difference between each measurement is <5%.

3. Results and discussion

3.1. Structural characterization

The hydrophilic and polycationic nature of CS in acidic media permit a good miscibility with MMT, and it can easily intercalate into the interlayers of the MMT by cationic exchange [16]. For this purpose, an acidic pH value is used to ionize the formation of $-NH_3^+$ groups in the CS structure. Given that the pK_a of the primary amine groups in the CS structure is 6.3, 95% of the amine groups will be protonated in the CS–MMT suspensions at pH 5. Fig. 1 illustrates the XRD patterns of neat MMT and CS–MMT suspensions with different CS–MMT ratios. The XRD pattern of the neat MMT (Fig. 1a) shows a reflection peak at about $2\theta = 6.5°$, corresponding to a basal spacing of 1.35 nm. The MMT in the suspension with the lowest CS-to-MMT ratio (0.5:1) shows a decrease in the 2θ value to about 5.6°, suggesting the intercalation of CS in a monolayer disposition (Fig. 1b). The lower 2θ value obtained for the MMT in the suspension with the highest CS-to-MMT ratio (2:1) is related to the intercalation of the CS as a bilayer (Fig. 1c). After ball-milling for 24 h, the XRD pattern of the MMT in the suspension shows a faint, broad peak at around $2\theta = 5$–6° (Fig. 1d). The broad peak with decreased intensity most likely indicated disordered, exfoliated and little intercalated MMT structures. In addition, it is hard to give a definitive conclusion regarding the nanostructural evolution through XRD analysis only without more convincing information. Recording the optical absorbance with time gives a suitable indication of the aggregation and sedimentation of the MMT in the suspensions. This method

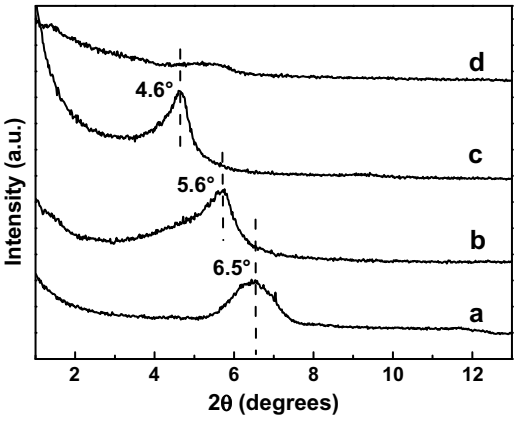

Fig. 1. Low-angle powder XRD patterns of (a) neat MMT, and CS–MMT nanocomposites with the CS–MMT ratios of (b) 0.5:1 and (c) 2:1, and (d) after ball-milling for 24 h.

allows us to distinguish accurately the difference in surface structures acquired by particle aggregates.

Fig. 2 shows the time dependence of the optical absorbance A (relative to its initial value, A_0) of the exfoliated MMT, original MMT and monolayer or bilayer intercalated-MMT suspensions. In theory [17], the sedimentation velocity U of interacting colloidal particles depends both on the hydrodynamic interactions mediated by the suspending solvent and on the microstructure of the suspension. In equilibrium, the latter is determined by direct potential forces arising, for example, from the steric repulsion between the particles and from the electrostatic repulsion of overlapping double layers. On the other hand, the long-range electrostatic repulsion occurring in suspensions of charged particles can give rise to a reduction in U, as compared with the dispersion of hard spheres at the same volume fraction. Watzlawek and Nägele [18] proposed a model in which the reduced sedimentation velocity of dilute deionized suspensions of weakly charged particles scaled according to $U/U_0 = 1 - p\psi^{1/2}$, where ψ is the particle volume fraction and U_0 is the sedimentation velocity at finite dilution, with a parameter p depending on the macroion charge Z ($p \propto |Z|^3$). Hence, it is believed from the time dependence of optical absorbance A (Fig. 2a) that the exfoliated MMT keeps a greater value of A/A_0 (~1) for a period of 180 min, due to it carrying more negatively charged sites on the surface layer, resulting in stronger electrical repulsion than that of non-exfoliated MMT. Nevertheless, the electrostatic attraction between ionized $-NH_3^+$ groups in the CS structure and negatively charged silicate layers neutralizes this repulsion force. It is thus expected that monolayer or bilayer intercalated-MMT (Fig. 2c) would exhibit faster sedimentation (lower values of A/A_0 after 180 min) than non-exfoliated MMT (Fig. 2b).

As shown in Fig. 3, it was found that the intensity of the diffraction peaks at $2\theta \sim 20°$, identified as semi-crystalline CS, decreased with the incorporation of MMT. Furthermore, the XRD patterns do not show any diffraction peak at $2\theta = 2$–$10°$, unlike the diffraction peak at $2\theta = 6.5°$ (d spacing = 1.35 nm) for original MMT, indicating the development of exfoliated silicate layers of MMT in CS matrix. It can be expected that the interaction between CS and exfoliated sheets ensures the formation of bonding in between, which further generates a strong cross-linking structure in the final nanohydrogels [13].

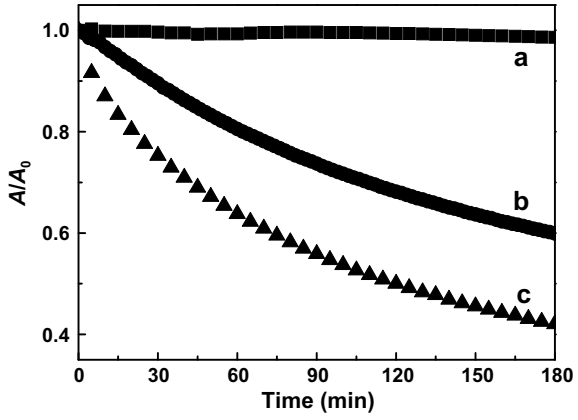

Fig. 2. Time dependence of optical absorbance A (relative to its initial value, A_0) of the (a) exfoliated MMT, (b) original MMT and (c) monolayer or bilayer intercalated-MMT suspensions.

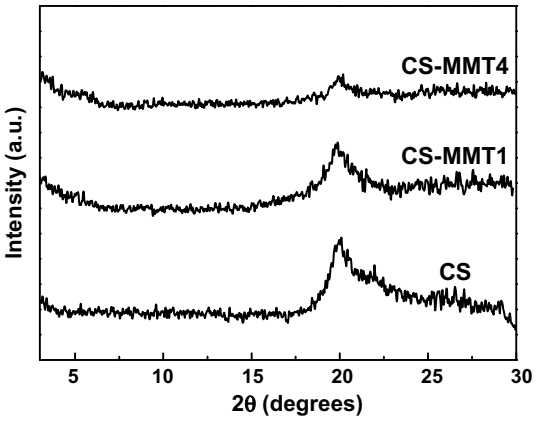

Fig. 3. Side-angle powder XRD patterns of pure CS, CS–MMT1 and CS–MMT4.

3.2. Drug release behavior under an applied electric field

Vitamin B_{12} is water soluble and has a low molecular weight (1355 Da). Its small molecular size and neutral charged state allows the molecule to be a suitable model drug for controlled release study in these nanohydrogels. Under a constant driving voltage (at 5 V), the time-dependent cumulative release of the drug from the nanohydrogels with different MMT concentrations revealed that both the release rate and the cumulative drug amount from pure CS hydrogel or the nanohydrogels upon electrostimulation are higher than that of pure CS with no applied electric field (Fig. 4a). This may be due to the ejection of drug from the electrosensitive hydrogels as a result of deswelling and syneresis [8]. In addition, it has to be mentioned that without electrostimulation the release rate of vitamin B_{12} from pure CS hydrogel is much closer to that of the nanohydrogels (the release profiles of vitamin B_{12} from the nanohydrogels are not shown). This suggests that nanoscale dispersion of MMT may not strongly influence the swelling of the CS matrix and the subsequent hindrance of the molecules from diffusion. In particular, this result is in good agreement with the fact that the MMT nanoplates were well dispersed in the CS matrix.

In order to further understand the drug release behavior of this nanohydrogel upon electrostimulation, the diffusion exponent n was determined using the power law [19]:

$$(M_t/M_o) = kt^n \quad (1)$$

where M_t is the amount of drug released at time t, M_0 is the amount of drug loaded during the preparation of the nanohydrogel, k is a rate constant and n is the diffusion exponent related to the diffusion mechanism. The changes of

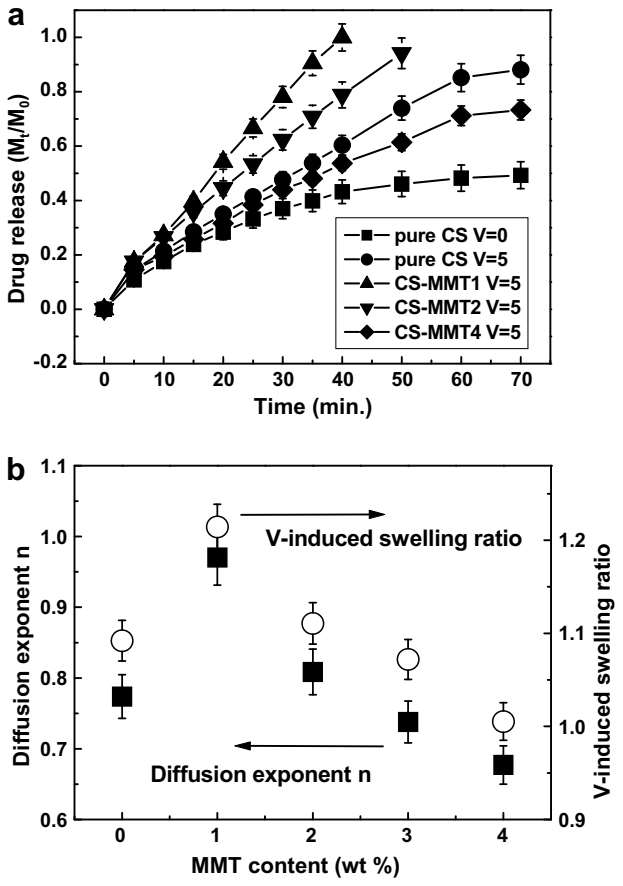

Fig. 4. (a) Time-dependent cumulative release curves of vitamin B_{12} from the nanohydrogels upon the application of an electric voltage, showing the different release profiles with different C_{MMT}. (b) Dependences of the loaded MMT contents on the diffusion exponent n and voltage-induced swelling ratios of the nanohydrogels. The filled boxes indicated the diffusion exponent n and the empty circles indicated the V-induced swelling ratio.

calculated values of n of the nanohydrogels with different C_{MMT} are shown in Fig. 4b. It is clear that the electrically controlled drug release behaviors of the nanohydrogels were changed with different amounts of MMT. It can be observed that the diffusion exponent n increased when 1 wt.% MMT was added to the pure CS. A small addition of MMT (1 wt.%) brings the n to a value close to 1, which indicates a change in drug release mechanism from diffusion-controlled to swelling-controlled mode. However, when MMT was continuously increased to 4 wt.%, the diffusion exponent n decreased. This decrease in n means a change in the drug release mechanism from swelling-controlled to diffusion-controlled. A plausible explanation can be deduced from our earlier study [12], where the incorporation of clay slightly deteriorated the crystallinity of CS whereas, in contrast, increasing the clay concentration in the CS matrix provided cross-linking bonds between the CS and clay. The influence of the increasing clay concentration is likely to be more pronounced in adding mechanical reinforcement to the nanohydrogel by increasing the cross-linked density, causing a decreased swelling ability. Moreover, the different degree of cross-linking will change the mesh size of the CS matrix sharply, resulting in various transport paths and diffusion velocities for the solute molecules.

The resulting equilibrium swelling ratios of the nanohydrogels with various MMT contents were seen to increase after applying electrostimulation, which hereinafter is defined as the voltage (V)-induced swelling ratio. Here, the V-induced swelling ratio can be appropriately estimated by the following equation:

$$\text{V-induced swelling ratio} = W_t/W_s \quad (2)$$

where W_t is the weight of the nanohydrogel swelling in PBS under an applied voltage of 5 V for 1 h and W_s is the equilibrium weight of the nanohydrogel swelling in PBS before electrostimulation. As shown in Fig. 4b, it was found that the ratio increases with a small addition of MMT (e.g. $C_{MMT} = 1$ wt.%) and then decreases with increasing C_{MMT}. It is thus suggested that the small MMT addition deteriorates the crystallinity of the nanohydrogel and enlarges the pore sizes in the CS matrix after electrostimulation. This nanostructural enlargement will increase the passage of ionic species and accelerate the drug release (and the rate) from the nanohydrogel, resulting in a pseudo-zero-order release under electrostimulation. In contrast, the higher cross-linking density as a result of a larger MMT addition retards the diffusion of the drug molecules across the nanohydrogel.

One interesting finding was that the effect of the MMT increment on the diffusion exponent n is very similar to that on the voltage-induced swelling ratio. As observed in Fig. 4b, both parameters show exactly the same dependence of the MMT concentration. Under an applied voltage of 5 V, the diffusion exponent n exhibits a linear correlation with the voltage-induced swelling ratio, with an R^2 as high as 0.99, indicating that the degree of cross-linking in the nanohydrogels due to the incorporation of MMT profoundly affects the drug diffusion behavior. This provides powerful evidence that the release of drug following electrostimulation is determined by the free volume in the matrix as the diffusion passage of molecules.

3.3. Repeating the effects of electrical stimulation on release behavior

A change in the electrical field has been shown to cause a change in the drug release profile. Therefore pulsatile patterns of drug release can be created by switching the electrical field off and on. Fig. 5 shows the resulting variation in the release profile of pure CS when a pulsatile release appeared immediately after an electrical field was applied, followed by little or negligible release of drug when the electrical field was removed, i.e. switched off. After several on–off switching operations, pure CS (solid curve) exhibited a decrease in responsiveness to the stimulation and in cumulative release amount compared with the ideal case (which should be able to maintain an identical release rate

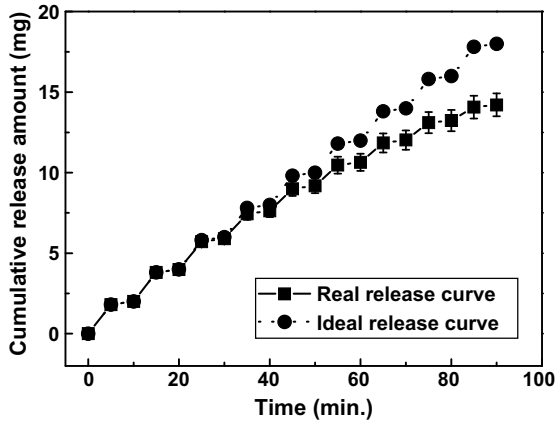

Fig. 5. Real (…) and ideal (—) pulsatile drug release profiles of pure CS hydrogels as an electric field was switched on and off.

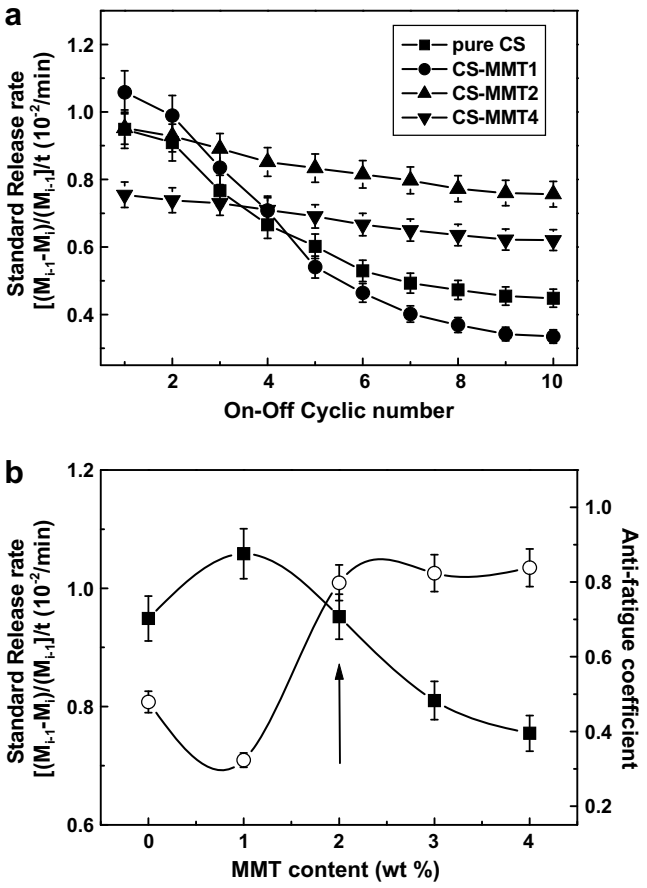

Fig. 6. (a) Standard release rates of drug from the nanohydrogels (CS, CS–MMT1, CS–MMT2 and CS–MMT4) after cyclic on–off switching operations. (b) Dependences of the loaded MMT contents on the drug standard release rate in the first on–off cycle (filled boxes) and anti-fatigue coefficient of the nanohydrogels (empty circles).

after repeated electrostimulation, i.e. a dotted curve), which is believed to be due to the fast swelling of the polymeric matrix caused by the stimulus.

In order to understand the mechanism that led to the decrease in responsiveness to electrostimulation after several on–off switching operations, the standard release rates (R_{sd}), as defined in the previous section, of the nanohydrogels with different C_{MMT} upon stimulation is plotted against the numbers of on–off switching cycles, as shown in Fig. 6a. Under an applied voltage, noticeable shrinkage of CS at the cathode occurred, presumably due to bulk solvent flow towards the anode. The H^+ ions formed by the electrolysis of water are subjected to intra- and intermolecular electrorepulsive forces arising from their interactions with adjacent H^+ ions and the positively charged CS network. These electrorepulsive interactions lead to an osmotic pressure gradient, which facilitates CS syneresis and ultimately results in gel shrinkage. Water, together with the dissolved drug, was expelled out of the hydrogel due to this contractile deformation. Moreover, the voltage-induced collapse after on–off switching operations leads to a decrease in ionizable groups (i.e. lower charged density) in pure CS, resulting in a decrease in the amount of the ions transported through the gel. As a result, for pure CS, a substantial decrease in release rate was exhibited with an increasing number of switching operations. In order to improve the anti-fatigue property of pure CS, the incorporation of MMT into the CS matrix, i.e. the nanohydrogel, effectively maintained the same capability of deswelling–swelling behavior after several cyclic switching operations, compared with the pure CS hydrogel [12].

Nanohydrogels with 1 wt.% MMT addition were observed to have a greater pulsatile release rate in the early stages (i.e. first two cycles) of operation, but after several on–off cycles (up to 10 cycles) its release rate slowed to less than that of pure CS. As mentioned above, the nanohydrogels with lower MMT addition (1 wt.%) deteriorated the crystallinity of CS and increase the passage of charge, thus enhancing the release rate of the model drug. Also, this deterioration of crystallinity weakened the strength of the nanohydrogels, which also reduced the responsiveness to electrostimulation (release rate) after cyclic on–off operations. However, with higher MMT concentrations (exceed 1 wt.% addition), stronger cross-linking in the nanohydrogels effectively improved the on–off cyclic responsiveness to electrostimulation, as shown in Fig. 6a. The release rate under electrostimulation is reduced because of the decrease in the molecular mobility in the nanohydrogels with the addition of MMT. Hence, it also suggested that the loose structure of the nanohydrogels (i.e. pure CS and the nanohydrogels with 1 wt.% MMT concentration) could hardly control the release in an effective manner following the electrostimulation protocol. However, this electrical-stimulus control can be effectively improved in the nanohydrogels with higher cross-link density, i.e. higher MMT concentrations. Both the initial release rate (R_1) and the relative anti-fatigue dependence of the MMT addition can be further plotted in Fig. 6b, in which the anti-fatigue coefficient was expressed as R_{10}/R_1, where R_1 and R_{10} indicate the standard release rate under on–off cycle numbers 1 and 10, respectively. A higher R_{10}/R_1 ratio means that the

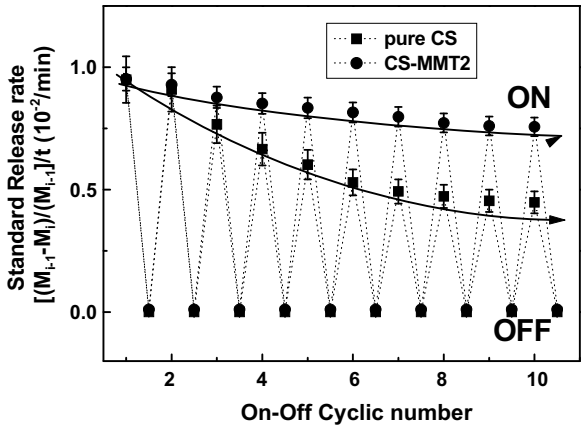

Fig. 7. Standard release rates of drug from pure CS and CS–MMT2 under cyclic on–off switching of electrostimulation.

nanohydrogel displays better anti-fatigue. Therefore, the optimal range of MMT content, typically around 2 wt.%, in the nanohydrogels is expected where the resulting nanostructure of the nanohydrogels can be well manipulated with optimal cross-linking density to keep the pulsatile release profile relatively constant even after numerous on–off switching operations. Fig. 7 shows a typical comparison of repeated on–off operations for pure CS and CS–MMT2 compositions, and suggests that the anti-fatigue property of CS can be largely improved with the incorporation of the MMT nanoplates. Such an improvement in the anti-fatigue behavior can be explicitly observed by the reversible mechanical action of the nanohydrogels upon cyclic switching under a given electrical stimulation. This constantly reversible action of the nanohydrogels also ensures a constant rate of pulsatile release of the drug, as shown experimentally, and this allows a more reliable consecutive pulsatile-type drug release profile to be achieved from such nanohydrogels.

4. Conclusion

A CS–MMT nanohydrogel responsive to electrostimulation was successfully prepared and systematically characterized in terms of crystallinity, anti-fatigue property and drug release behavior. The exfoliated silica sheets act as cross-linkers to form a strong network structure between the CS and MMT. Under an applied voltage, the drug release behavior was strongly influenced by the concentration of MMT, which affected the cross-linking density of the nanohydrogels. Vitamin B_{12} displays pseudo-zero-order release kinetics and the release mechanism shifted from being diffusion-controlled to being swelling-controlled mode when a low MMT content (1 wt.%) was added. However, with an MMT content exceeding 1 wt.%, both the diffusion exponent n and the responsiveness to electrical stimulation were decreased. Furthermore, the resulting nanostructure of the nanohydrogels can be successfully manipulated to keep the pulsatile release profile relatively constant after repeated on–off switching operations. In this study, the nanohydrogel with 2 wt.% MMT addition was demonstrated to exhibit excellent anti-fatigue behavior and better pulsatile release compared with pure CS. This new class of nanohydrogels provides an interesting alternative as a long-standing electrically induced drug delivery system with reliable drug release performance.

Acknowledgement

This work was financially supported by the National Science Council of the Republic of China, Taiwan under Contract of No. NSC-95-2221-E-009-126.

References

[1] Rodriguez-Cabello JC, Prieto S, Reguera J, Arias FJ, Ribeiro A. Biofunctional design of elastin-like polymers for advanced applications in nanobiotechnology. J Biomat Sci-Polym E 2007;18:269–86.
[2] Gupta KM, Barnes SR, Tangaro RA, Roberts MC, Owen DH, Katz DF, et al. Temperature and pH sensitive hydrogels: an approach towards smart semen-triggered vaginal microbicidal vehicles. J Pharm Sci 2007;96:670–81.
[3] Peteu SF. Responsive materials configured for micro- and nanoactuation. J Intel Mat Syst Str 2007;18:147–52.
[4] Lin CC, Metters AT. Hydrogels in controlled release formulations: network design and mathematical modeling. Adv Drug Deliver Rev 2006;58:1379–408.
[5] Chen SB, Singh J. In vitro release of levonorgestrel from phase sensitive and thermosensitive smart polymer delivery systems. Pharm Dev Technol 2005;10:319–25.
[6] Hoffman AS. Intelligent polymers. In: Park K, editor. Controlled drug delivery: challenges and strategies. Washington, DC: American Chemical Society; 1997.
[7] Yang Y, Engberts JBFN. Stimuli response of polysoap hydrogels in aqueous solution and DC electric fields. Colloid Surf A: Physicochem Eng Aspects 2000;169:85–94.
[8] Sutani K, Kaetsu I, Uchida K. The synthesis and the electric-responsiveness of hydrogels entrapping natural polyelectrolyte. Radiat Phys Chem 2001;61:49–54.
[9] Liang L, Liu J, Gong X. Thermosensitive poly(*N*-isopropylacrylamide)–clay nanocomposites with enhanced temperature response. Langmuir 2000;16:9895–9.
[10] Wang SF, Shen L, Tong YJ, Chen L, Phang IY, Lim PQ, et al. Biopolymer chitosan/montmorillonite nanocomposites: preparation and characterization. Polym Degrad Stabi 2005;90:123–31.
[11] Ramanathan S, Block H. The use of chitosan gels as matrices for electrically-modulated drug delivery. J Control Release 2001;70:109–23.
[12] Liu K-H, Liu T-Y, Chen S-Y, Liu D-M. Effect of clay content on electrostimuli deformation and volume recovery behavior of clay–chitosan hybrid composite. Acta Biomater 2007;3:919–26.
[13] Haraguchi K, Farnworth R, Ohbayashi A, Takehisa T. Compositional effects on mechanical properties of nanocomposite hydrogels composed of poly(*N*,*N*-dimethylacrylamide) and clay. Macromolecules 2003;36:5732–41.
[14] Darder M, Colilla M, Ruiz-Hitzky E. Chitosan–clay nanocomposites: application as electrochemical sensors. Appl Clay Sci 2005;28:199–208.
[15] Kim SY, Lee YM. Drug release behavior of electrical responsive poly(vinyl alcohol)/poly(acrylic acid) IPN hydrogels under an electric stimulus. J Appl Polym Sci 1999;74:1752–61.

[16] Darder M, Colilla M, Ruiz-Hitzky E. Biopolymer–clay nanocomposites based on chitosan intercalated in montmorillonite. Chem Mater 2003;15:3774–80.
[17] Xu W, Nikolov A, Wasan DT. The effect of many-body interactions on the sedimentation of monodisperse particle dispersions. J Colloid Interface Sci 1998;197:160–9.
[18] Watzlawek M, Nägele G. Sedimentation of strongly and weakly charged colloidal particles: prediction of fractional density dependence. J Colloid Interface Sci 1999;214:170–9.
[19] Peppas NA. Analysis of Fickian and non-Fickian drug release from polymers. Pharm Acta Helv 1985;60:110–1.